J. Plasma Physics (1997), *vol.* 58, *part* 2, *pp.* 223–232. Printed in the United Kingdom

© 1997 Cambridge University Press

Three-dimensional nonlinear mode coupling of the double-tearing instability

X. H. DENG, J. F. WANG, B. C. ZHANG and Z. G. CHEN

Department of Space Physics, Wuhan University, Wuhan, 430072, People's Republic of China

(Received 1 February 1996)

The nonlinear development of the double-tearing instability and the mode coupling of different helicities are investigated numerically in cylindrical geometry. The results show that double-tearing instability arises with a central-hollow current-density profile, and the coupling of different low-poloidal mode numbers m leads to rapid destabilization of modes with higher poloidal mode numbers. This instability ultimately leads to the resistive reconnection of parts of the fluxes and reduces the current gradient in the unstable region. It seems likely that this process would accelerate current penetration in the tokamak start-up phase, and it also possibly plays an important role in the triggering of solar flares.

1. Introduction

Tearing instability plays an important role in many astrophysical (Priest 1985) and laboratory (White 1986) plasma processes. The tearing mode with sufficient amplitude leads to magnetic reconnection (Carreras *et al.* 1978), and its nonlinear development can result in global reconfiguration of magnetic topology and can account for the conversion of large amounts of magnetic energy.

Since the single-tearing mode grows relatively slowly and saturates early (Rutherford 1973), some attention has been paid to mechanisms for further nonlinear development. The first suggestion concerns the overlappings of the resonances. The magnetic islands from different layers interact nonlinearly and accelerate the loss of confinement (Waddell *et al.* 1978). Another suggestion is that, assuming the short-wavelength excitations to be initially dominant, the islands will spontaneously coalesce to long wavelengths (Finn and Kaw 1977; Pritchett and Wu 1979; Biskamp and Welter 1980). In the absence of instability, the normal current penetration time of tokamaks is of the order of $\mu_0 a^2/\eta$. If the current rise is sufficiently slow compared with this time, the current profile is peaked around the plasma axis. If, however, the current rise is faster, a skin current is formed. In addition, Parker (1974) has shown that a current-carrying flux loop emerging from subphotospheric regions of the Sun may lead to the current forming a skin profile on the outside of the loop. On the other hand, the interaction of two loops with large current may result in the formation of a large global system, in which the total current density profile has a double-peaked structure. Double-tearing instability will develop, and islands are formed on adjacent rational surfaces in the plasma has multiple rational

https://doi.org/10.1017/S0022377897005606 Published online by Cambridge University Press

surfaces ($\mathbf{k}\cdot\mathbf{B}=0$ at more than one location) and two singular surfaces are in close proximity. In this paper we study numerically the nonlinear development of the double-tearing instability and the mode coupling of different helicities with a central-hollow current-density profile in cylindrical geometry. The possible implications of this process for fast current penetration in the tokamak start-up phase and the triggering of solar flares is discussed.

2. Fundamental equations

We start from the following resistive magnetohydrodynamic equations:

$$\frac{\partial\rho}{\partial t}+\nabla\cdot(\rho\mathbf{V})=0, \tag{1}$$

$$\rho\left[\frac{\partial\mathbf{v}}{\partial t}+(\mathbf{v}\cdot\nabla)\,\mathbf{v}\right]=-\nabla P+\mathbf{J}\times\mathbf{B}+\rho\nu\nabla^2\mathbf{v}, \tag{2}$$

$$\mathbf{J}=\frac{\nabla\times\mathbf{B}}{\mu_0}, \tag{3}$$

$$\frac{\partial\mathbf{B}}{\partial t}=-\nabla\times\mathbf{E}, \tag{4}$$

$$\mathbf{E}+\mathbf{v}\times\mathbf{B}=\eta\mathbf{J}, \tag{5}$$

where ρ, $\mathbf{v}$, P, $\mathbf{J}$, $\mathbf{B}$ and $\mathbf{E}$ are the plasma mass density, the velocity, the pressure, the current density, the magnetic field and the electric field; μ_0, ν and η are the vacuum magnetic permeability, the viscosity and the resistivity respectively.

For simplicity, we assume that the equilibrium magnetic field B_z is uniform and much larger than other magnetic components, and that the plasma pressure is smaller than the magnetic pressure ($\beta=2p/B_z^2\ll 1$). These assumptions are appropriate for solar applications (Parker 1972), and incompressibility with constant isotropic resistivity is valid for the double-tearing instability (Ofman 1992). The magnetic field $\mathbf{B}$ and the plasma velocity $\mathbf{v}$ may be taken as

$$\mathbf{B}=\nabla\psi\times\mathbf{e}_z+B_{z0}\,\mathbf{e}_z, \tag{6}$$

$$\mathbf{V}=\nabla\phi\times\mathbf{e}_z, \tag{7}$$

where ψ and ϕ are the z components of the potential function of $\mathbf{B}$ and the stream function of $\mathbf{V}$. All physical quantities are written in dimensionless form, and the resulting equations are (Strauss 1976)

$$\left(\frac{\partial}{\partial t}+\mathbf{V}\cdot\nabla\right)u=\mathbf{B}\cdot\nabla J_z+\nu\nabla_\perp^2\,u, \tag{8}$$

$$\frac{\partial\psi}{\partial t}=\mathbf{B}\cdot\nabla\phi-\eta J_z+E_z, \tag{9}$$

where $J_z=-\nabla_\perp^2\,\psi$, $u=-\nabla_\perp^2\,\phi$, $\nabla_\perp=\nabla-\mathbf{e}_z\,\partial/\partial z$, u is the toroidal component of the vorticity, and the subscript $\perp$ indicates the component perpendicular to the toroidal magnetic field.

3. Computational procedures and numerical results

In this paper we chose a central-hollow current-density profile with a constant plasma density and resistivity, and study the nonlinear evolution of the double-

https://doi.org/10.1017/S0022377897005606 Published online by Cambridge University Press

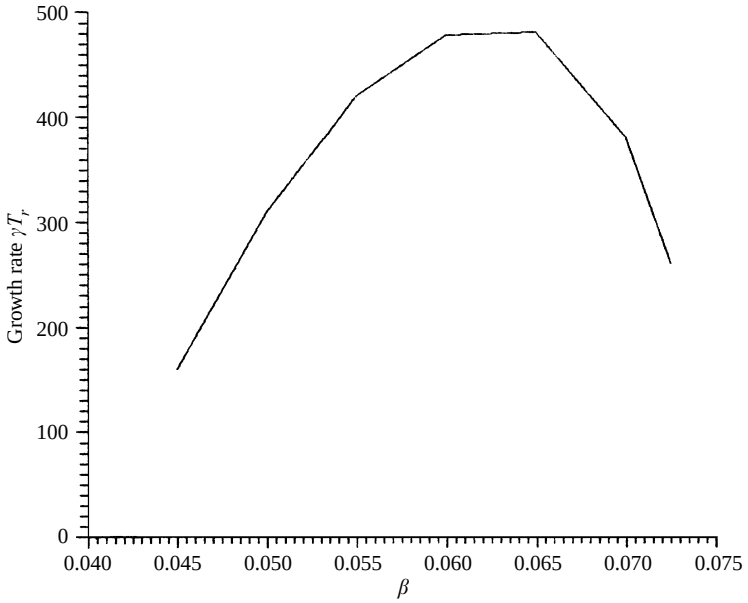


Figure 1. The normalized growth rate γT_r of the 2/1 mode as a function of β, with $S = 10^4$, $q(0) = 7.0$, $q(1) = 6.0$ and $\alpha = 1$ kept fixed.

tearing mode and the mode coupling of different helicities in a long and thin standard cylinder. The safety factor q can be written in the form (Schnack and Killeen 1979)

$$q(r) = q(0)\,\beta\frac{[1+(r/r_0)^{2\alpha}]^{1+\alpha}}{\beta+(r/r_0)^{2\alpha}}, \tag{10}$$

where $q(0)$, β, α and r_0 are free parameters.

The equations are solved using a nonlinear, initial-value computer code (Deng and Wang 1992), employing a partial–implicit algorithm and the predictor–corrector method. We make Fourier expansions in the poloidal and toroidal coordinates and a difference form in the radial direction; more than 51 modes are considered, and 301 points are taken in the radial direction. The time step satisfies the numerical stability condition (Richtmyer and Morton 1967)

$$\Delta t \leqslant \frac{2R}{aS\max|n-m/q|}, \tag{11}$$

where $S = T_r/T_a$ is the magnetic Reynolds number, with $T_r = a^2/\eta$ and $T_a = a/C_a$, a and R are the minor and major radii of the torus, and m and n are the poloidal and toroidal mode numbers respectively.

When the q profile has the same rational value at two points on the minor radius, a pair of magnetic islands form with the same helicity, and will develop in a sequence of flux contours. In the single-mode case and for a safety-factor q profile with $q(0) = 7.5$, $q(1) = 5.94$, $R_0 = 0.28$, $\beta = 0.06$ and $\alpha = 1.5$, it is shown that the 2/1 and 3/2 modes become unstable, while the 4/3 and 5/3 modes remain stable. For $m/n = 2/1$, when the separation of the two rational surfaces is large, the pair of islands will grow to a certain width and then remain constant in time; this means that the islands have reached a state of saturation. This situation is similar to the behaviour of $m \geqslant 2$ modes in the single-helicity case with monotonically decreasing current profiles, and the growth rate is

https://doi.org/10.1017/S0022377897005606 Published online by Cambridge University Press

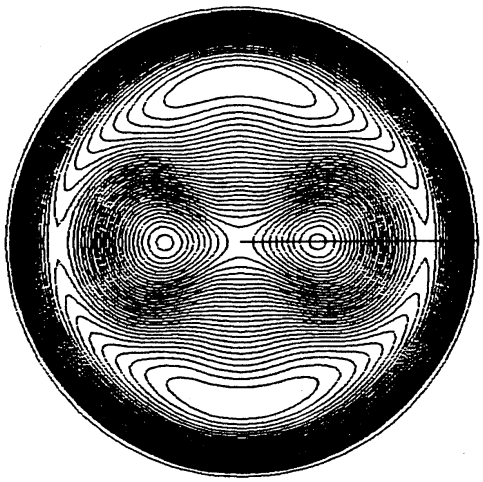


Figure 2. The helical flux function ψ contour in the $z = 0$ plane for the $m/n = 2/1$ mode.

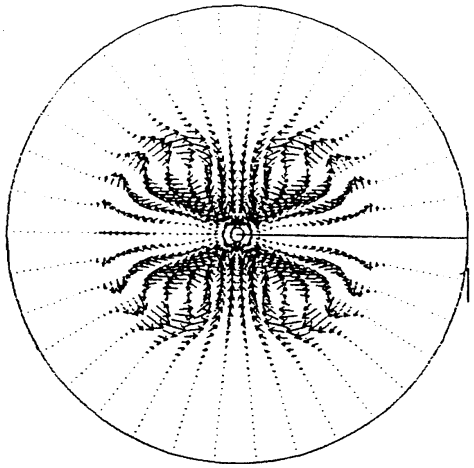


Figure 3. The distribution of the disturbed plasma velocity in the $z = 0$ plane for the $m/n = 2/1$ mode.

predicted to scale as $S^{-3/5}T_a^{-1}$. But when the separation of the two rational surfaces is small, the two islands can interact actively, and the growth rate is much faster than that of the slow modes. The perturbed flux function ψ varies considerably across the singular layers, and the structure of the mode proves to be essentially identical with that of the fast $m = 1$ tearing mode for a peaked current profile. This means that the constant-ψ approximation is badly violated, and the growth rate makes a transition from a $S^{-3/5}T_a^{-1}$ to a $S^{-1/3}T_a^{-1}$ scaling. This result is in partial agreement with that of Pritchett *et al.* (1980). In Fig. 1 we give out the growth rate γT_r of the 2/1 mode as function of β with $S = 10^4$, $q(0) = 7.0$, $q(1) = 6.0$ and $\alpha = 1$ kept fixed. The basic reason why multiple-tearing modes with close separation of the rational layers result in such fast reconnection rates is the presence of a convective flow pattern, which is set up by the reconnection. In Figs 2 and 3 the contours of the helical flux function ψ and the distribution of the disturbed plasma velocity for the $m/n =$

https://doi.org/10.1017/S0022377897005606 Published online by Cambridge University Press

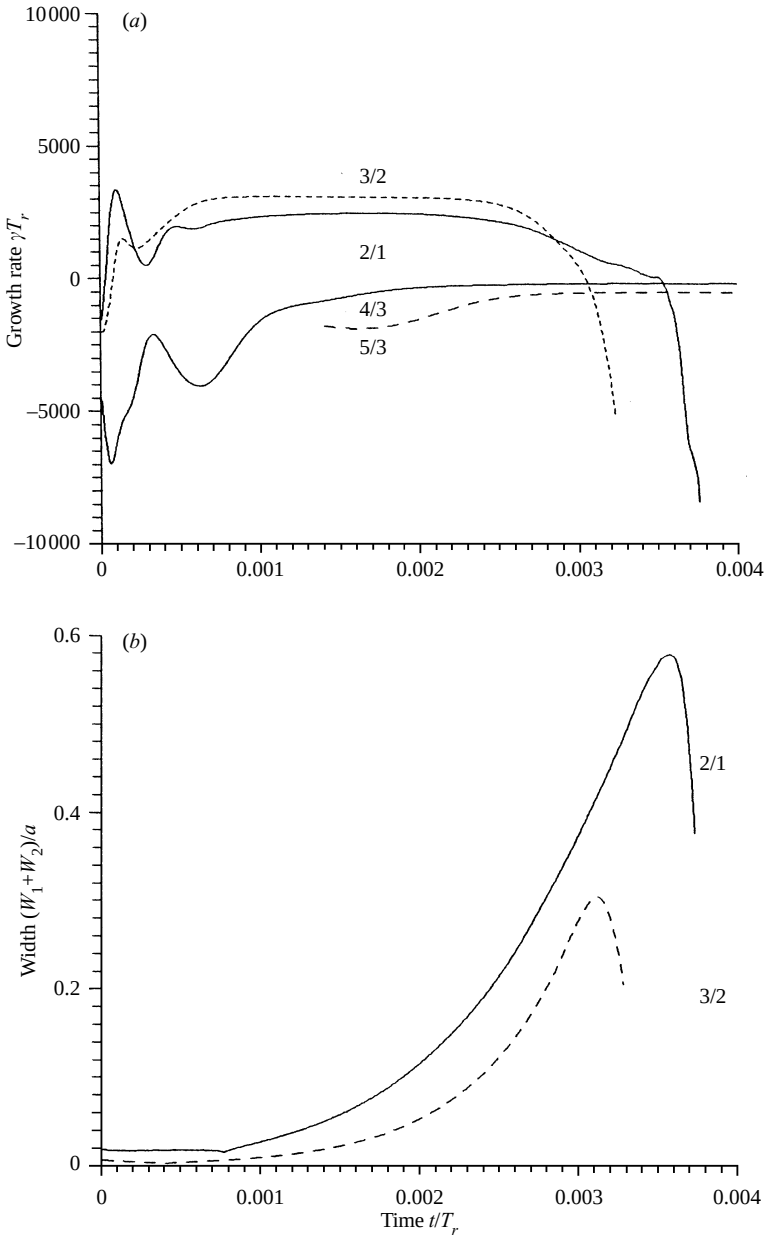


Figure 4. The normalized growth rates γT_r of the 2/1, 3/2, 4/3 and 5/3 modes versus time (a) and the total width W_1+W_2 for each pair of islands (b) in the single-helicity case with $S = 10^4$, $q(0) = 7.5$, $q(1) = 5.94$, $R_0 = 0.28$, $\beta = 0.06$ and $\alpha = 1.5$.

2/1 mode are illustrated. It can be seen that the interaction between adjacent singular surfaces leads to enhanced vortex and magnetic field distortion in the region between the surfaces. The radial components of both the velocity and the magnetic field are large over the entire region between the singular surfaces. The perturbation is not limited to the singular layer about each surface, but is more evenly distributed. This increased radial flow convects more magnetic

https://doi.org/10.1017/S0022377897005606 Published online by Cambridge University Press

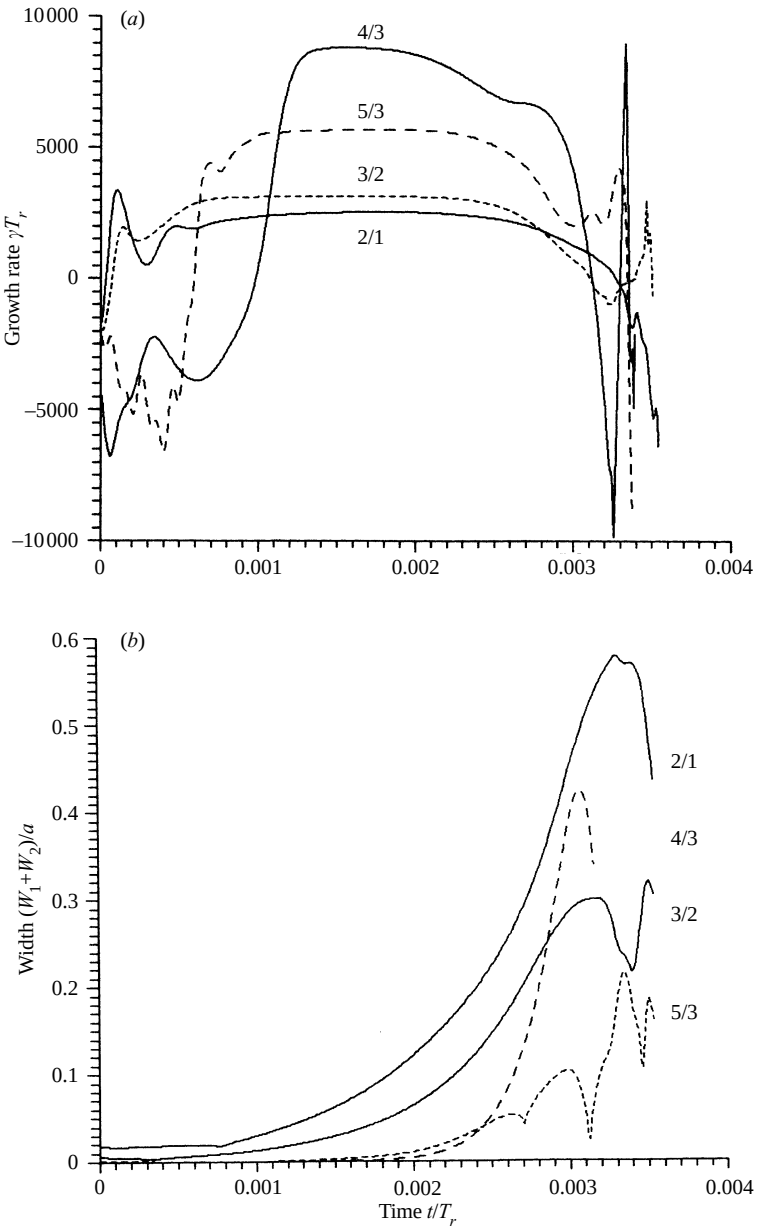


Figure 5. The normalized growth rates γT_r of the 2/1, 3/2, 4/3 and 5/3 modes versus time (a) and the total width $W_1 + W_2$ for each pair of islands (b) in the multiple-mode-coupling case with $S = 10^4$, $q(0) = 7.5$, $q(1) = 5.94$, $R_0 = 0.28$, $\beta = 0.06$ and $\alpha = 1.5$.

field into the reconnection region of each singular surface, so that the linear growth rate of the double-tearing mode is greatly enhanced over that of the single-tearing mode.

In the mode-coupling case that considers the nonlinear mode coupling of different helicities, significant changes in the evolution of the 4/3, 5/3 and other modes with higher poloidal mode numbers take place. Instead of being stable, they are driven unstable and grow quickly through the processes of mode

https://doi.org/10.1017/S0022377897005606 Published online by Cambridge University Press

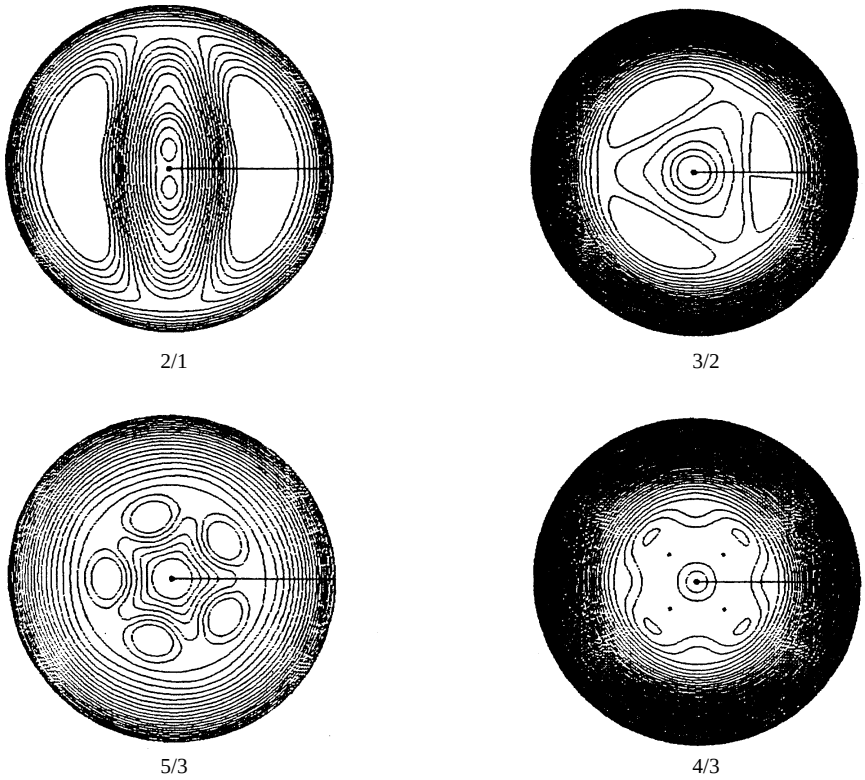


Figure 6. The helical flux function ψ contour in the $z = 0$ plane for the 2/1, 3/2, 4/3 and 5/3 modes in the multiple-mode-coupling case.

coupling. In Figs 4 and 5 we give the normalized growth rates γT_r for the 2/1, 3/2, 4/3 and 5/3 modes versus time, and correspondingly the total width $W_1 + W_2$ for each pair of islands in both the single-mode case and the multiple-mode-coupling case respectively, with $S = 10^4$, $q(0) = 7.5$, $q(1) = 5.94$, $R_0 = 0.28$, $\beta = 0.06$ and $\alpha = 1.5$. It is interesting to note that at the nonlinear stage, the 3/2, 4/3 and 5/3 modes are further destabilized and the growth rates exhibit strong peaks at a time of about $t = 0.0032T_r$. We can see that in the multiple-helicity-coupling case, although the total width of the pair of islands of the 2/1 mode is almost unchanged, the total width of the 4/3 mode is larger than that of the 3/2 mode, and the total widths of the 3/2 and 5/3 modes become almost comparable.

Figures 6 and 7 display the magnetic-island configurations for the 2/1, 3/2, 4/3 and 5/3 modes and the corresponding distributions of velocity fields respectively. It can be seen that in the multiple-helicity-coupling case the total configurations for the magnetic field and the velocity field are given by the overlapping of the magnetic fields and the velocity fields of modes with different helicities. Such overlapping of sets of magnetic islands on adjacent rational surfaces would bring about relatively rapid reconnection of magnetic lines of force, and could cause a sudden redistribution of the plasma current. This process may also produce tearing-mode turbulence and lead to anomalous resistivity (Stix 1976; White *et al.* 1977), which can further accelerate the development of tearing instabilities and enhance magnetic field reconnection.

https://doi.org/10.1017/S0022377897005606 Published online by Cambridge University Press

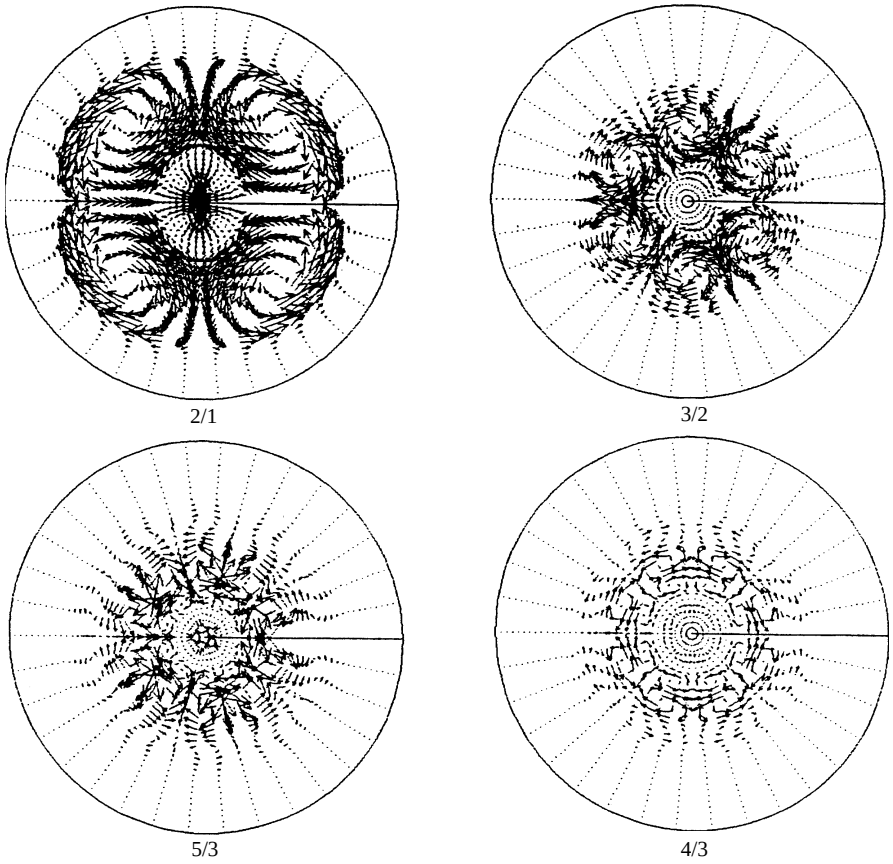


Figure 7. The distributions of the velocity fields for the 2/1, 3/2, 4/3 and 5/3 modes corresponding to Fig. 6.

Increasing the number of modes and changing the value of S can only modify the results to some extent, but does not change the basic dynamical mechanism and the global tendency.

4. Discussion and conclusions

In this paper the nonlinear evolution of the double-tearing instability and the mode coupling of different helicities has been investigated numerically in cylindrical geometry. The results clearly show that the double-tearing mode is unstable with a hollow current-density profile. The linear growth rate of the double-tearing mode can be greatly enhanced when the two singular surfaces are in close proximity, and is predicted to scale as $S^{-1/3}T_a^{-1}$. This is due to strong convection of the field into the reconnection region of each singular surface. The nonlinear coupling of tearing modes with low-poloidal mode numbers m leads to rapid destabilization of the modes with higher poloidal mode numbers, and results in an enormous increase in the number of magnetic neutral points, accompanied by an increase in the rate of magnetic field dissipation.

Current penetration in the early stage of a tokamak discharge is observed to be much faster than the classically expected rate based on resistive diffusion

https://doi.org/10.1017/S0022377897005606 Published online by Cambridge University Press

(Dimock *et al.* 1973), and the existence of high-m and high-l magneto-hydrodynamic activity (Granetz *et al.* 1979) in this phase has prompted several authors to explain the observed rates in terms of enhanced transport caused by micro-instabilities (Hitchcock *et al.* 1981). In the tokamak start-up phase, the plasma current flows in a narrow region near the plasma edges, where it gives rise to a safety factor q profile very different from the normal one increasing monotonically with minor radius. It is suggested that the initial rapid current penetration of the tokamak discharge may be attributed to the nonlinear mode coupling of the double-tearing instability, which causes growth and overlap of radially separated magnetic islands. It is suggested that the ensuing reconnection and braiding of magnetic lines would enhance local radial heat and particle transport, and could permit rapid redistribution of the plasma current; this process may also account for the observed high-m and high-l magneto-hydrodynamic activity in the tokamak start-up phase.

Observations and studies have shown conclusively that the interaction of current loops is an essential ingredient in the triggering of solar flares (Sakai 1989). Parker (1974) has shown that a current-carrying flux loop emerging from subphotospheric regions may lead to the current forming a skin profile on the outside of the loop. In addition, the interaction of two loops with large current could possibly result in the formation of a large global system in which the total current density profile may have a double-peaked structure. Double-tearing instability is driven by the current gradient, and can develop when $\mathbf{k}\cdot\mathbf{B} = k_z B_z + (m/r) B_\theta = 0$ occurs in two different places (note that m and k_z may have negative or positive values). In this case double-tearing instabilities can be excited and grow at a fast rate in these interconnecting loops, within which sufficient magnetic free energy is stored. Because the tearing mode is a long-wavelength mode, it will lead to the observed substantial brightening of a loop along much of its length, as well as the brightening of interconnecting loops. But it must be pointed out that, for application of the process to explain the triggering of solar flares, more detailed observational analysis of the evolution of current systems associated with flares is urgently needed, and more complete and accurate calculations are necessary before a loop–flare model can be obtained.

Acknowledgements

We should like to thank the Editor Professor George H. Miley for encouragement and the two referees for valuable suggestions to improve the paper. This project is supported by the Natural Science Foundation of China.

References

Biskamp, D. and Welter, H. 1980 *Phys. Rev. Lett.* **44**, 1069.

Carreras, B. A., Waddell, B. V., Hicks, H. R. and Lynch, S. J. 1978 *Phys. Rev.* **A18**, 2732.

Deng, X. H. and Wang, S. 1992 *The Magnetic and Velocity Fields of Solar Active Regions. Proceedings of IAU Colloquium* No. 141 (ed. H. Zirin, G. X. Ai and H. M. Wang), p. 433. Astronomical Society of the Pacific.

Dimock, D. L., Eubank, H. P., Hinnov, E., Johnson, L. C., Furth, H. R., Rutherford, P. H. and Selburg, H. 1973 *Phys. Fluids* **16**, 1054.

Finn, J. M. and Kaw, P. V. 1977 *Phys. Fluids* **20**, 72.

Granetz, R. S., Hutchinson, I. H. and Overskei, D. O. 1979 *Nucl. Fusion* **19**, 1587.

https://doi.org/10.1017/S0022377897005606 Published online by Cambridge University Press

Hitchcock, D. A., Mahajan, S. M. and Hazeltine, R. D. 1981 *Phys. Fluids* **24**, 2.

Ofman, L. 1992 *Phys. Fluids* **B4**, 2751.

Parker, E. N. 1972 *Astrophys. J.* **174**, 499.

Parker, E. N. 1974 *Astrophys. J.* **191**, 245.

Priest, E. R. 1985 *Rep. Prog. Phys.* **48**, 955.

Pritchett, P. L. and Wu, C. C. 1979 *Phys. Fluids* **22**, 2140.

Pritchett, P. L., Lee, Y. C. and Drake, J. F. 1980 *Phys. Fluids* **23**, 1368.

Richtmyer, R. D. and Morton, K. W. 1967 *Difference Methods for Initial Value Problems.* Interscience, New York.

Rutherford, P. H. 1973 *Phys. Fluids* **16**, 1903.

Sakai, I.-J. 1989 *Solar Phys.* **20**, 117.

Schnack, D. D. and Killeen, J. 1979 *Nucl. Fusion* **19**, 877.

Stix, T. H. 1976 *Phys. Rev. Lett.* **36**, 521.

Strauss, H. R. 1976 *Phys. Fluids* **19**, 134, 1976.

Waddell, B. V., Carreras, B. A., Hicks, H. R., Holmes, J. A. and Lee, D. K. 1978 *Phys. Rev. Lett.* **41**, 1386.

White, R. B. 1986 *Rev. Mod. Phys.* **58**, 183.

White, R. B., Montocello, D. A., Rusenbluth, M. N. and Waddell, B. A. 1977 *Phys. Fluids* **20**, 800.

https://doi.org/10.1017/S0022377897005606 Published online by Cambridge University Press